Avian magnetoreception model realized by coupling a magnetite-based mechanism with a radical-pair-based mechanism*

Lü Yan(吕 琰)[a] and Song Tao(宋 涛)[a)b)†]

[a] Beijing Key Laboratory of Bioelectromagnetism, Institute of Electrical Engineering, Chinese Academy of Sciences, Beijing 100190, China
[b] France–China Bio-Mineralization and Nano-Structures Laboratory (BioMNSL), Beijing 100190, China

(Received 8 August 2012; revised manuscript received 15 October 2012)

Many animal species have been proven to use the geomagnetic field for their navigation, but the biophysical mechanism of magnetoreception has remained enigmatic. In this paper, we present a special biophysical model that consists of magnetite-based and radical-pair-based mechanisms for avian magnetoreception. The amplitude of the resultant magnetic field around the magnetic particles corresponds to the geomagnetic field direction and affects the yield of singlet/triplet state products in the radical-pair reactions. Therefore, in the proposed model, the singlet/triplet state product yields are related to the geomagnetic field information for orientational detection. The resultant magnetic fields corresponding to two materials with different magnetic properties are analyzed under different geomagnetic field directions. The results show that ferromagnetic particles in organisms can provide more significant changes in singlet state products than superparamagnetic particles, and the period of variation for the singlet state products with an included angle in the geomagnetic field is approximately 180° when the magnetic particles are ferromagnetic materials, consistent with the experimental results obtained from the avian magnetic compass. Further, the calculated results of the singlet state products in a reception plane show that the proposed model can explain the avian magnetoreception mechanism with an inclination compass.

Keywords: magnetoreception, orientation, geomagnetic field, magnetic particles, radical pair

PACS: 87.50.–a, 87.50.dc, 02.90.+p **DOI:** 10.1088/1674-1056/22/4/048701

1. Introduction

Various animals use the geomagnetic field for their navigation. The use of the magnetic compass by migratory birds was first described in European robins.[1] In the following years, it has been further demonstrated in more than 50 species.[2] Recently, two most convincing biophysical mechanisms of magnetoreception in birds have been proposed: a magnetite-based mechanism[3–5] and a radical pair-based mechanism.[6–8]

The magnetite-based mechanism is established on the discoveries that magnetic particles are widely found in bacteria and higher organisms.[9–12] These magnetic particles were suggested to be involved in magnetoreception, and verified by various biophysical methods. Some magnetite-based models have been presented and theoretically evaluated to explain magnetoreception.[13–17]

The model proposed by Kirschvink[13] and Kirschvink *et al*.[14] was based on the presumption that the magnetic particles in organisms are single-domain (SD) magnetites. The authors believed that the external magnetic field exerts a magnetic torque on the particle, which rotates the particle to open or close the ion channel and produces nerve signals. The model presented by Davila *et al*.[15] was based on superparamagnetic (SP) nanoparticles. They assumed that the SP nanoparticles can be magnetized, and the local magnetic field in the cell is amplified by orders of magnitude under the external magnetic field. Thus, magnetic particles experience an attractive or repulsive force to induce their displacement, which can induce a primary receptor potential via strain-sensitive membrane channels to create nerve signals. Fleissner *et al*.[16] and Solov'yov and Greiner[17] analyzed the magnetoreception process in birds using two types of ferromagnetic magnetite particles based on the model given by Davila *et al*.[15] All the models mentioned above indicate that nerve signals are transmitted through the ophthalmic branch of the trigeminal nerve to the brain, and magnetic fields are used as a compass or component of a navigational "map" for the navigation of birds.[18,19]

However, these theories cannot explain the light dependence of magnetic orientation confirmed by several behavioral experiments.[20–22] Further, Zapka *et al*.[23] reported that European robins with a bilateral section in the ophthalmic branch of the trigeminal nerve can still use their magnetic compass for orientation, which is in conflict with the magnetite-based mechanism because the mechanism requires trigeminal nerve signal transmission.

On the other hand, the radical-pair-based mechanism is established on the premise that weak magnetic fields can affect spin-related free-radical recombination reactions.[24–28] The

*Project supported by the State Key Program of the National Natural Science Foundation of China (Grant No. 51037006), the State Key Development Program for Basic Research of China (Grant No. 2011CB503702), and the Young Scientists Fund of the National Natural Science Foundation of China (Grant No. 51207155).

†Corresponding author. E-mail: songtao@mail.iee.ac.cn

© 2013 Chinese Physical Society and IOP Publishing Ltd

singlet/triplet radical-pair product can act as the receptor of the external magnetic field, and migratory birds can use it to sense changes in the geomagnetic field. The magnetosensitivity of the radical-pair reaction must be anisotropic to detect the direction information of the geomagnetic field using the radical-pair mechanism.

Theoretically, the molecules that provide the radical pairs can possess the required properties to produce the anisotropic effect.[29,30] Thus, Ritz *et al*.[31] proposed a special structure of radical pairs called "reference-probe" design, where the internal magnetic field of the "reference" radical should be much higher than the external field, but the "probe" radical has very small or no internal magnetic field. Lau *et al*.[32] suggested that the molecules that play host to the magnetically sensitive radical-pair intermediate must be immobilized and rotationally ordered within receptor cells. Then, a partially rotational disorder can cause anisotropic responses to differently oriented radical pairs within the same cell. Although an anisotropic radical-pair magnetic field effect has been observed in several solutions or liquid crystal experiments,[33–38] no direct evidence in the sense of a microcosmic mechanism has been obtained until now. Moreover, the isotropic response to radical pairs has been identified in cryptochrome recently,[39] but the reporter wonders whether the cryptochrome is sufficient for the purpose as a chemical magnetoreceptor, because its magnetic sensitivity seems to be a general feature of this protein family.

In addition, some research work reported on the radical pairs subjected to magnetic fields produced by iron-containing particles and structures.[40–45] The present view in the field also suggests that the combined mechanism might be more sensitive. However, the previous studies about the combined mechanism still need to improve.[46] Binhi[41] speculated that the rate of intracellular free-radical biochemical reaction will be changed by stray fields produced in different orientations by the intracellular magnet, which was thought of as an indirect torque-transduction pathway for magnetoreception by Winklhofer and Kirschvink,[47] who believed that the model can explain the conflicting results reported by Zapka *et al*.[23] To achieve maximum angular sensitivity, the Binhi compass model requires that the intracellular magnet should rotate, and the magnet should be coupled to a soft elastic matrix. Cohen[43] and Yang and Cohen[44] demonstrated how magnetic nanostructures can catalyze intersystem crossings in molecular radical pairs. The radical pair was assumed to be randomly distributed and randomly oriented on the surface of the magnetic nanostructure. Cohen *et al*. modeled the nanostructure as a uniformly magnetized sphere to calculate the magnetic field gradient at the surface of the sphere. The effect of the geomagnetic field on the magnetic field gradient near the magnetic nanostructures was not considered. Cai *et al*.[45] illustrated the relationship between the quantum entanglement and the sensitivity of the chemical compass for magnetoreception. They especially demonstrated how to optimize the design of a chemical compass using a much better directional sensitivity by simply employing a gradient field created in the vicinity of a hard ferromagnetic nanostructure. They assigned directly the value of the gradient field to analyze the magnetic field sensitivity of the chemical compass without considering the real structure of the nanoparticles in birds.

In this paper, the equivalent model of magnetic particles is established based on the real nanoparticle structure in birds. A special combination of magnetite-based and radical-pair-based mechanisms is analyzed to evaluate the justifiability of the model. In contrast to existing models, the present model adopts the amplitude of the resultant magnetic field around the magnetic particles (but not the magnetic field gradient) to represent the geomagnetic field direction. Based on the amplitude variation of the resultant magnetic field, the singlet state product yield of the reactions is calculated using the radical-pair mechanism. Thus, product yield is related to the geomagnetic field information.

2. Combined mechanism

The equivalent model of the magnetic particles in birds is based on the physical–chemical measurement results. The magnetic field induced by the magnetic particles and the geomagnetic field produce a magnetic resultant field, whose amplitude depends on the spatial location and the direction of the geomagnetic field. Hence, the directional change in the geomagnetic field can be represented by the resultant magnetic field amplitude.

According to the radical-pair mechanism, the radical pair $D^+ + A^-$ is created by an electron transferred from donor molecule D to acceptor molecule A. The spin directions of radical pair $D^+ + A^-$ have an anti-parallel alignment, and the spin state is called singlet state; when the alignment is parallel, it is called a "triplet state". The radical pair originates from a singlet state; its singlet and triplet states are interconverted by hyperfine interaction, and the process is affected by the applied magnetic field. Therefore, the product yield of a singlet/triplet state varies with the change in the resultant magnetic field arising from the change in the geomagnetic field direction. The radical-pair product yield is thus related to the geomagnetic field information. Consequently, variation in the product yield will change the number of neurotransmitters, thus resulting in an increase or a decrease of the signal in the nerve cell that receives the neurotransmitters for navigation. However, the mechanism for transduction of the change from singlet-triplet state to cell membrane depolarization is still unclear. Some research suggested that the cryptochrome may act as a potential

primary magnetoreceptor to receive the information about the change in the radical-pair product yields.[7]

The proposed mechanism can well explain the questions that are difficult to answer by the magnetite-based or radical-pair-based mechanism only. Dealing with the role of the magnetic particles in changing the direction information of the geomagnetic field into amplitude of the resultant magnetic field is the core of the proposed model. Previous relevant research has not considered this option. Furthermore, because the equivalent model of magnetic particles was established based on real bird nanoparticle structures, if more convictive experimental evidence for anisotropic interaction of radical pairs is obtained from future works, this mechanism can also be used to analyze the effect of magnetic particles, which exist universally in migrant birds,[48] on the radical-pair product yield.

3. Calculation model

According to the μ-SXRF (synchrotron-based X-ray fluorescence) experiment on paraffin section series taken from the upper beak skin of the homing pigeon, the iron-containing structure has three subcellular components: chains of maghemite crystals, magnetite clusters, and the iron-coated vesicle,[16] as shown in the upper left corner of Fig. 1(a). To analyze the resultant magnetic field produced by the interaction between the magnetic particles and the geomagnetic field, the iron-containing structure in the upper beak that contains magnetic particles is simulated as a cylinder. The cylinder length is designated as $l = 300$ μm, and the diameter is designated as $D = 10$ μm, by evaluating the sizes of the magnetic particles and the dendrites of the homing pigeon's beak[10] as shown in Fig. 1(a). It should be pointed out that this experimental result has been disputed recently. The new ultrastructure studies show that the magnetic particles are in the form of macrophages, not magnetosensitive neurons.[49] However, all research in the field has identified that the magnetic particles actually exist in the pigeon's beak. Therefore, the principle remains unchanged. Considering the lack of the biophysical experimental data about the size of the iron-containing structure in birds, it is meaningful to establish the equivalent model of the magnetic particles based on this structure.

The x axis is defined as the central axis of the cylinder, the y axis is perpendicular to the central axis of the cylinder, and the z axis is perpendicular to the xy plane and parallel to the left and right surfaces of the cylinder. This rough assumption is not suitable for quantitative calculation because of insufficient biophysical experimental data, but it is sufficient for qualitative analysis of the effects of the resultant magnetic field on the radical pair product yield. To investigate the resultant magnetic field distribution, curve l_1 in the xy plane and curve l_2 in the xz plane, shown in Fig. 1(a), are chosen to calculate the amplitude of the resultant magnetic field at different positions when the applied magnetic field changes. a_1–b_1 and a_2–b_2 and d_1–e_1 and d_2–e_2 are line segments parallel to the x axis; the distance from o' (centerpoint of the left surface of the cylinder) to the line is ±0.4 mm. b_1–d_1 and b_2–d_2 are arcs each with a radius of 0.4 mm and an angle of 180°, whose centerpoint is o'.

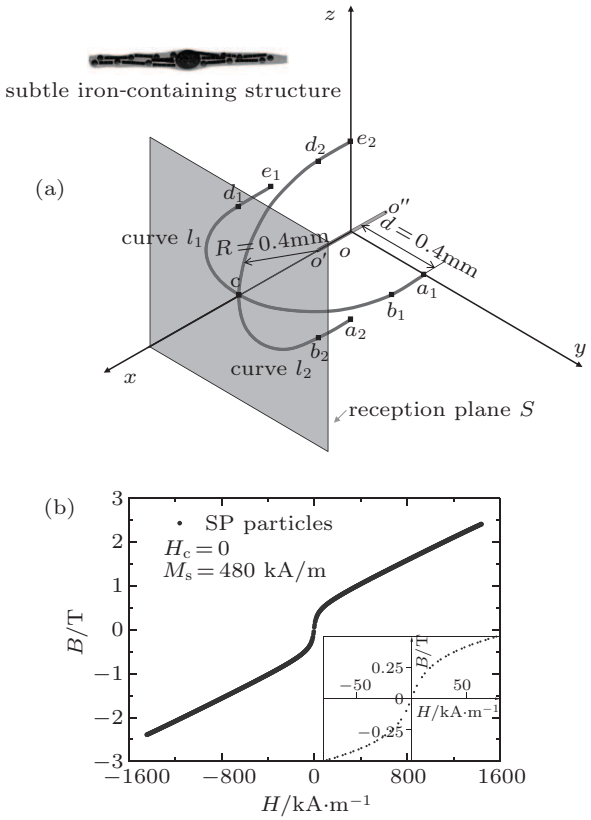


Fig. 1. Magnetic field calculation. (a) Three-dimensional model for magnetic particles. The cylinder is used to simulate the magnetic particles in birds. The center of the cylinder is the origin of the coordinate system for calculation. (b) Experimental B–H curve of the SP nanoparticles measured by VSM.

For the convenience of calculation, the bird body is assumed to be parallel to the x axis of the reference coordinate system. Therefore, when the bird changes its angle of flight attitude, the direction of the geomagnetic field (not the bird body) would rotate in the reference frame. Magnetic field $\boldsymbol{B}_{\rm ext}$, whose included angle θ with respect to the x axis changes from $-180°$ to 180°, is applied as a boundary condition to simulate the geomagnetic field. Assuming that magnetic field $\boldsymbol{B}_{\rm ext}$ is in the xz plane, then the x component of the external magnetic field will be $B_{{\rm ext}_x} = B_0 \cos\theta$, the y component $B_{{\rm ext}_y} = 0$, and the z component $B_{{\rm ext}_z} = B_0 \sin\theta$, where $B_0 = |\boldsymbol{B}_{\rm ext}| = 50$ μT. With regard to the magnetic material properties, two kinds of magnetic materials are proposed to be involved in the magnetoreception process, i.e., SP nanoparticles and ferromagnetic materials.

(i) SP nanoparticles: This proposal is based on the findings of the SP nanoparticles in birds using transmission electron microscope (TEM) imaging in bright and dark-field mode and using small-area electron diffraction (SAED).[4] The SP particles, whose coercivity is close to zero, were considered as an amplifier of the geomagnetic field in the magnetoreception process. Considering the lack of measurement results of the specific properties of magnetic particles in birds, the experimental results of the SP nanoparticle (diameter: 10 nm, produced by Ferrotec Corporation, Japan) are used to determine the magnetic properties. The B–H curve shown in Fig. 1(b) is measured using a vibrating sample magnetometer (VSM). The coercivity of the SP material for the magnetic field calculation obtained from the B–H curve is zero, and the relative permeability is 16. The measurement sample of the SP nanoparticle is a magnetic fluid and not pure SP nanoparticles. To obtain the magnetic properties of the SP materials, the curve is amplified using the saturation magnetization of Fe_3O_4 ($M_s = 480$ kA/m).

(ii) Ferromagnetic materials: This proposal is based on the findings of two different types of iron compounds in the upper beak skin of adult homing pigeons using different light and electron microscopic methods combined with X-ray analysis. These two iron compounds are identified to be two ferromagnetic materials: magnetite and maghemite,[16] which closely resemble the real iron-containing structure in birds. Technically, these two types of materials are ferromagnetic, but have different structural properties from ferromagnetic ores. However, the specific magnetic properties of the two types of materials have not been identified by measurements yet. In comparison with the SP materials, the coercivity of the ferromagnetic materials for magnetic field calculation is set to be 17 kA/m, and the relative permeability is assumed to be 16. In addition, the residual magnetization direction of the magnetic cylinder is considered to be along the x axis (i.e., central axis of the cylinder). These parameters are almost the same as those used in the magnetic particle simulation model given by Solov'yov and Greiner.[17]

The resultant magnetic fields corresponding to these two kinds of magnetic materials are calculated and used to analyze the product yield of the radical pair. As this analysis is performed through a large-scale qualitative simulation, the assumption for the two magnetic materials does not consider the special characteristics of the magnetic particles on a nanometer scale. The isotropic radical-pair magnetic field effect is used to calculate the singlet state product yield of the reactions under different magnetic field strengths using the method given by Timmel and Henbest.[50] This method is considered in the case of a radical pair with a single spin-1/2 nucleus (e.g., a proton), in which radical-pair diffusion is ignored and singlet/triplet pairs are allowed to disappear according to the first-order kinetics with rate constants $k_S = k_T = k$.[51] The formula for calculating the singlet state product yield Φ_S is shown in Eq. (1), where ω is the Larmor frequency ($\omega = \gamma B$) and a is the isotropic hyperfine coupling constant, and is given as

$$\begin{aligned}\Phi_S = {} & \frac{3}{8} + \frac{1}{8}\cdot\frac{\omega^2}{\Omega^2} + \frac{1}{8}\cdot\frac{a^2}{\Omega^2}\cdot f(\Omega) \\ & + \frac{1}{8}\cdot\left(1-\frac{\omega}{\Omega}\right)\cdot f\left(\frac{1}{2}a+\frac{1}{2}\omega+\frac{1}{2}\Omega\right) \\ & + \frac{1}{8}\cdot\left(1-\frac{\omega}{\Omega}\right)\cdot f\left(\frac{1}{2}a-\frac{1}{2}\omega-\frac{1}{2}\Omega\right) \\ & + \frac{1}{8}\cdot\left(1+\frac{\omega}{\Omega}\right)\cdot f\left(\frac{1}{2}a-\frac{1}{2}\omega+\frac{1}{2}\Omega\right) \\ & + \frac{1}{8}\cdot\left(1+\frac{\omega}{\Omega}\right)\cdot f\left(\frac{1}{2}a+\frac{1}{2}\omega-\frac{1}{2}\Omega\right). \end{aligned} \tag{1}$$

In addition, $f(x)$ is the Lorentzian function, where

$$f(x) = \frac{k^2}{k^2+x^2}, \tag{2}$$

$$\Omega = (a^2+\omega^2)^{1/2}. \tag{3}$$

4. Calculation results

4.1. Magnetic field distribution

The relationships between the amplitude of the resultant magnetic field $|B|$, the included angle θ between the applied magnetic field and the central axis of the magnetic cylinder, and length L_i in curves l_1 and l_2, calculated in the cylindrical magnet of SP and the ferromagnet are shown in the three-dimensional (3D) diagram in Fig. 2. L_i is defined as the length from point a_i in curve l_i ($i = 1, 2$). When θ is 0°, the $|B|$ distribution corresponding to distance L_1 in curve l_1 is the same as that of L_2 in curve l_2 because of axial symmetry as shown in Figs. 3(a) and 3(b). The relationship between $|B|$ and d_x (distance from o' to the calculation point at the x axis) is shown in Fig. 3(c).

To investigate the effect of the change in magnetic field amplitude ($\Delta|B| = |B|_{max} - |B|_{min}$, where $|B|_{max}$ is the maximum value of $|B|$ and $|B|_{min}$ is the minimum value of $|B|$) on the product yield of a radical pair, the values of $|B|$ at centerpoint c in curves l_1 and l_2 (i.e., $L_i \approx 800$ μm) in the SP and ferromagnetic materials are calculated. This process also compares the difference between the two materials. The relationships between $|B|$ and θ in the SP and ferromagnetic materials with $d_x = 0.4$ mm are shown in Figs. 4(a) and 4(b), respectively ($\Delta|B|_{SP} \approx 0.03$ μT and $\Delta|B|_{Ferromagnet} \approx 24$ μT).

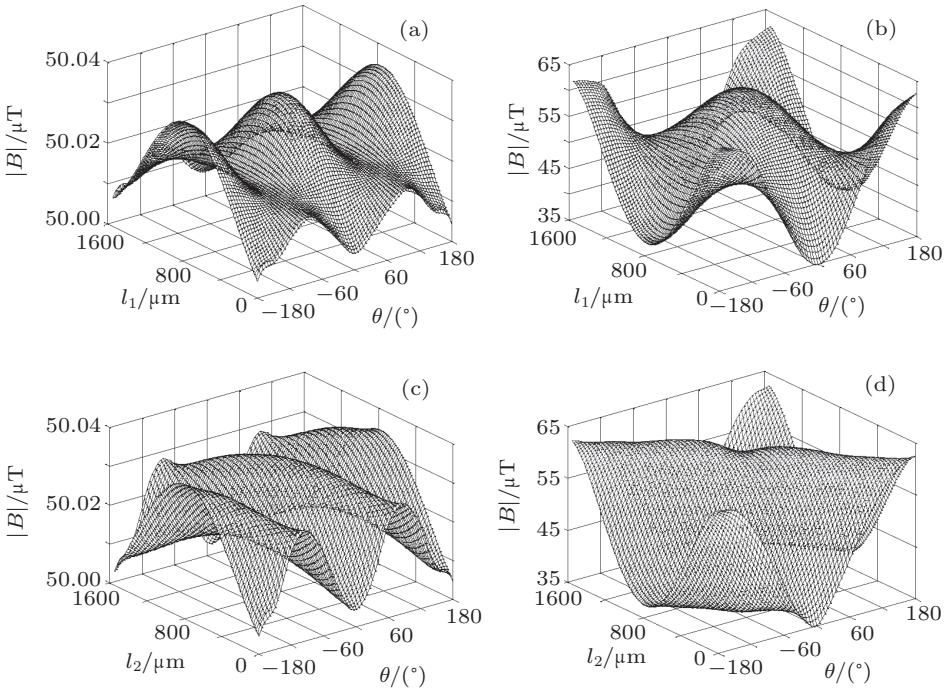


Fig. 2. Resultant magnetic field $|B|$ distribution when θ varies from $-180°$ to $180°$, showing relationships between $|B|$, θ, and the position of the observed point in curve l_1 in the SP material (a) and the ferromagnetic material (b), and those in curve l_2 in the SP material (c) and the ferromagnetic material (d).

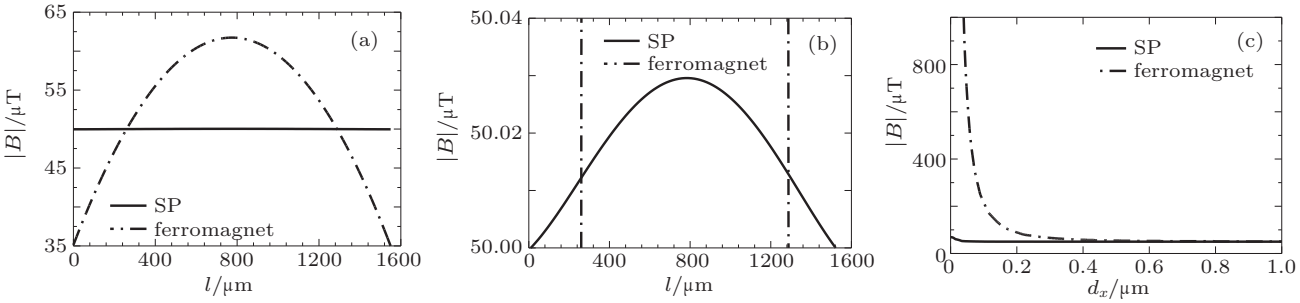


Fig. 3. Distribution of $|B|$ at different positions when $\theta = 0°$. (a) Distribution of $|B|$ along curve l_1 or l_2. (b) Partial enlargement of Fig. 3(a). (c) Distribution of $|B|$ along the x axis.

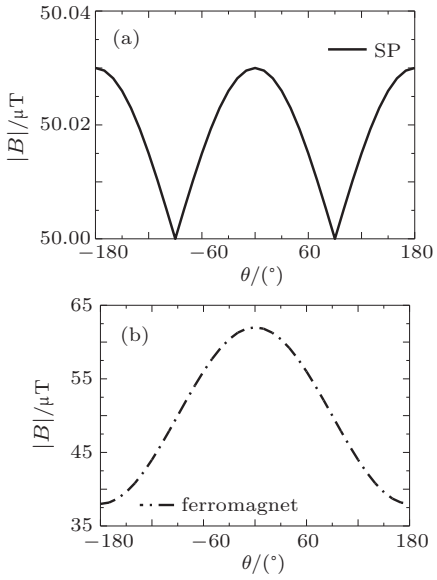


Fig. 4. Relationships between $|B|$ and θ at $d_x = 0.4$ mm for SP material (a) and ferromagnetic material (b).

4.2. Singlet state product yield corresponding to the magnetic field

The singlet state product yield Φ_S is calculated according to the method mentioned in Section 3. The relationship between the singlet state product yield Φ_S and $|B|$ is shown in Fig. 5(a). To facilitate discussion, the horizontal axis considered in the figure is $|B|$ but not $|B|/a$, although the latter is more commonly used in other papers. In addition, based on the experimental results in a protein environment using flash photolysis,[52] the decay rate k is set to be 1 μs^{-1}. According to the calculation formula, the different values of hyperfine coupling constant a affect the Φ_S range corresponding to the change in the magnetic field direction angle θ from $-180°$ to $180°$ located in different parts of the curve as shown in Figs. 5(b) and 5(c). If a is much higher than the Larmor frequency of $|B|$, the Φ_S range corresponding to the magnetic field direction angle θ monotonically decreases as shown by

the dashed line ($a = 3.0\ \mu s^{-1}$) in Fig. 5(a). The relationships between Φ_S and θ in the SP and the ferromagnetic materials are shown by the dashed lines in Figs. 5(b) and 5(c), respectively. If a is much lower than the Larmor frequency of $|B|$, the Φ_S range corresponding to the magnetic field direction angle θ monotonically increases as shown by the dot–dashed line ($a = 1.6\ \mu s^{-1}$) in Fig. 5(a). The relationships between Φ_S and θ in the SP and ferromagnetic materials are shown by the dot–dashed lines in Figs. 5(b) and 5(c), respectively. If the value of a is appropriate, the Φ_S range can also include the turning point as shown by the solid line ($a = 2.1\ \mu s^{-1}$) in Fig. 5(a). Under this condition, the relationships between Φ_S and θ in the SP and ferromagnetic materials are shown by the solid lines in Figs. 5(b) and 5(c), respectively.

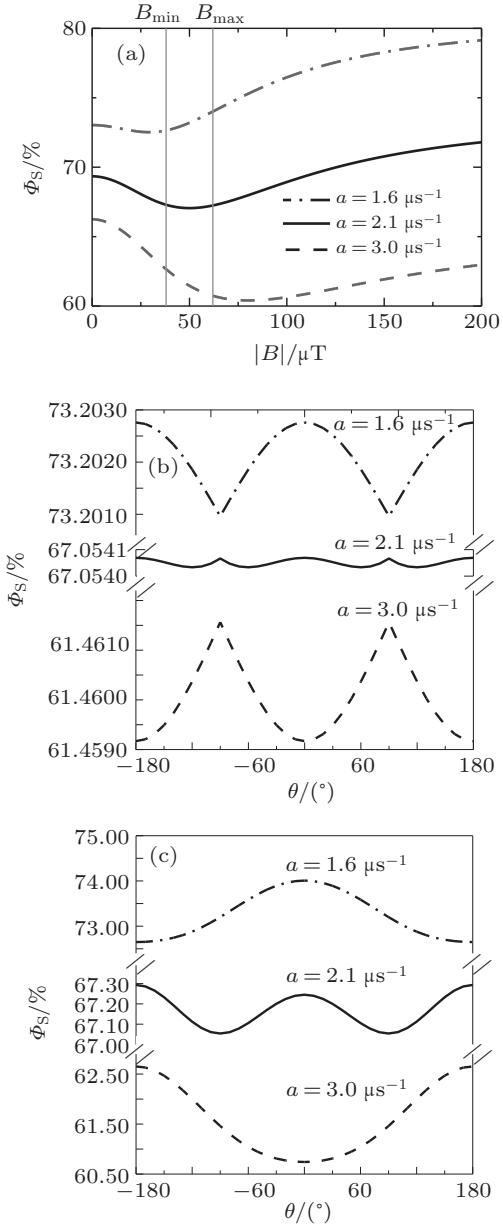


Fig. 5. Variations in the singlet state product yield Φ_S of the radical pairs, showing (a) relationship between Φ_S and B/a, (b) relationship between Φ_S and θ in the SP material, and (c) relationship between Φ_S and θ in the ferromagnetic material.

4.3. Modulation patterns corresponding to the geomagnetic information

The results presented above only indicate the variation of Φ_S corresponding to the magnetic field direction at a specific point. Generally, the sensory receptors of organisms are assumed to have ordered structures; thus, a reception plane is chosen to investigate the singlet state product yield distribution of the ferromagnetic material in this section. Assuming that the residual magnetization direction of the magnetic cylinder is along the bird body axis, the sensory receptors are arranged in reception plane S (area: 0.5 mm×0.5 mm) parallel to the yz plane. The distance of reception plane S along the positive direction of the x axis from o' is 0.4 mm, as shown by the gray quadrangle in Fig. 1(a). According to the proposed model, when the applied magnetic field rotates in the direction parallel to the xy and xz planes (the included angle θ with respect to the x axis changes from 0° to 180°), the Φ_S distribution corresponding to $|B|$ is calculated as shown in Fig. 6.

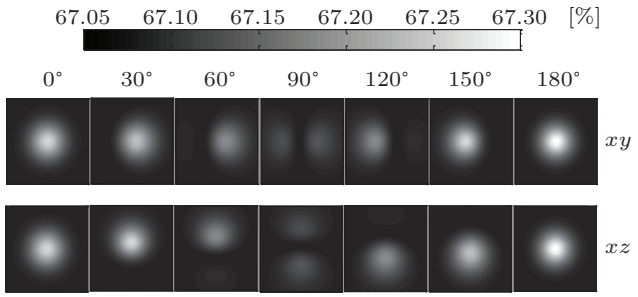


Fig. 6. Modulation patterns of Φ_S through the magnetic field parallel to the xy and xz planes in different directions at angles 0°, 30°, 60°, 90°, 120°, 150°, and 180°.

5. Discussion

By using the combined mechanisms in this paper, we investigated the amplitude of the resultant magnetic field around the magnetic particles instead of the magnetic field gradient, which is different from the research by Cohen and Cai. This process means that the changes in the singlet state product yields correspond directly to the magnetic field at the same spatial position, and the difference in local magnetic field between the two radicals of each radical pair is ignored. This result can be attributed to the difference in local magnetic field between the two radicals, which is much smaller than the change in the resultant magnetic field amplitude $\Delta|B|$ during the geomagnetic field rotation in the proposed mechanism. For example, when the distance from the magnetic particles $d_x = 0.4$ mm, $\Delta|B|_{SP} \approx 0.03\ \mu T$, and $\Delta|B|_{ferromagnet} \approx 24\ \mu T$. If the distance between two radicals is 3.5 nm (the same as the value used in Cai's calculation[45]), the difference in the local magnetic field between the two radicals is approximately $5.29\times10^{-5}\ \mu T$. Even the distance from the magnetic particles is reduced to $d_x = 10\ \mu m$, the variation is still very small

(6.02×10^{-2} μT). In Cai's calculation, it was approximately 4 mT, considerably larger than our calculation result, which is possibly because Cai assumed that the acceptor of the radical pairs was 35 nm away from the magnetic particles. Therefore, the proposed model appears more reasonable in the case where the distance between the radical pairs and the magnetic particles is relatively far.

Based on the calculation results of magnetic field distribution, $|B|$ is found to change cyclically with included angle θ, and the period of variation was 180° in the SP material and 360° in the ferromagnetic material. When θ is 0°, the values of $|B|$ at centerpoint c in the two kinds of materials both reach the maximum values. The $|B|_{\rm SP}$ varies in a manner similar to the function $f(\theta) = |\sin(\theta - 90^\circ)| + \text{offset}$. The $|B|_{\rm ferromagnet}$ variation at centerpoint c is in the form similar to a cosine wave with an offset because ferromagnetic material has inherent remanence, whereas SP material does not have such property.

In the calculation, $\Delta|B|_{\rm SP}$ is very small because $|B|$ decays exponentially with d_x increasing; if d_x is smaller, then $\Delta|B|_{\rm SP}$ would become higher. For example, if $d_x = 0.1$ mm, then $\Delta|B|_{\rm SP} \approx 0.3$ μT ($\Delta|B|_{\rm ferromagnet} \approx 250$ μT). If $d_x = 10$ μm, then $\Delta|B|_{\rm SP} \approx 20$ μT ($\Delta|B|_{\rm ferromagnet} \approx 8800$ μT). In all cases, the variation trends of $|B|$ in the SP material with different values of d_x are almost similar. Therefore, the calculation result with $d_x = 0.4$ mm can still be used for qualitative analysis.

At the same spatial position as point c in Fig. 1(a), $|B|_{\rm ferromagnet}$ is much larger than $|B|_{\rm SP}$. The change in the singlet state product yields $\Delta\Phi_{\rm S} = \Phi_{\rm Smax} - \Phi_{\rm Smin}$ of the ferromagnetic material, which is also much larger than $\Phi_{\rm S}$ of the SP material. When $d_x = 0.4$ mm ($\Delta|B|_{\rm SP} \approx 0.03$ μT and $\Delta|B|_{\rm ferromagnet} \approx 24$ μT), the decay rate is $k = 1$ μs^{-1}, and the values of hyperfine coupling constant a are 1.6, 2.1, and 3.0 μs^{-1}. The calculated $\Delta\Phi_{\rm S}$ of the SP material are approximately 1.8×10^{-5}, 3.6×10^{-7}, and 2.4×10^{-5}, and the values of $\Delta\Phi_{\rm S}$ of the ferromagnetic material are approximately 1.36%, 0.24%, and 1.91%, respectively. The changes in product yields $\Phi_{\rm S}$ calculated at present are relatively small. If d_x decreases slightly (but not below micrometer level), then $\Delta\Phi_{\rm S}$ would become more significant. For example, when $d_x = 0.1$ mm, $\Delta\Phi_{\rm S}$ of the SP material corresponding to the same values of hyperfine coupling constant a of 1.6, 2.1, and 3.0 μs^{-1} would be approximately 1.8×10^{-4}, 1.2×10^{-6}, and 2.4×10^{-4}, respectively ($\Delta|B|_{\rm SP} \approx 0.3$ μT). The values of $\Delta\Phi_{\rm S}$ of the ferromagnetic materials are approximately 6.56%, 3.03%, and 2.59%, respectively ($\Delta|B|_{\rm ferromagnet} \approx 250$ μT), which means that the reception radical pairs are not too far from the magnetic particles, especially not probably located so far as the retina of the birds, according to the proposed mechanism.

We can reasonably assume that nature has optimized the properties through evolution to provide maximum results; therefore, these calculation results can explain why biophysical experiments showed that the magnetic particles in organisms are more similar to ferromagnetic (and not SP) materials.[16] The former can provide more significant changes in product yield $\Phi_{\rm S}$, which makes magnetoreception more feasible.

Moreover, when the range of singlet state product yield $\Phi_{\rm S}$ includes a turning point in the ferromagnetic material or the $\Phi_{\rm S}$ range monotonically decreases or increases in the SP material, the values of $\Phi_{\rm S}$ corresponding to the magnetic field direction angle $\theta = 0^\circ$ and $\theta = 180^\circ$ both attain the maxima (the values are almost equal), indicating that the magnetic compass is an inclination compass. This conclusion is in agreement with the experimental results obtained from a variety of research activities on migratory birds,[53] where the formula for calculating the singlet state product yield $\Phi_{\rm S}$ is based on one-proton radical pair. In fact, when the radical pairs are more complex, the calculation formula will also become more complex. However, the curve of $\Phi_{\rm S}$ corresponding to $|B|$ also has an extreme value; therefore, the proposed model is still suitable.

In addition, because the experimental results show that the properties of the magnetite crystals in birds are more similar to ferromagnetic materials, SD (single-domain) magnetic materials were not considered in the model calculation. In fact, SD magnetic material will only make the magnetic field around the magnetic particles higher and, hence, inducing more significant changes in the product yield, but the variation trend of $\Phi_{\rm S}$ calculated with SD material is still similar to that obtained with the ferromagnetic material.

Based on the response pattern of the singlet state product yield $\Phi_{\rm S}$, the geomagnetic information is found to be represented by the distribution of $\Phi_{\rm S}$ in the reception plane. The position of high $\Phi_{\rm S}$ is located at the central position of the reception plane because the body axis is parallel to the geomagnetic field. If the included angle between the body axis and the geomagnetic field is changed in the horizontal or vertical plane, the position of the high $\Phi_{\rm S}$ will move correspondingly along the horizontal or vertical direction. The pattern for a bird flying in the direction anti-parallel to the magnetic field direction (180°) is similar to the pattern for parallel orientation (0°), which also demonstrates that the magnetic compass of the bird is intrinsically an inclination compass. Birds can use modulation patterns to adjust the flight direction.

The previous discussions ignored the rotation of the bird itself around the body axis during the flight, which often happens in the bird altitude adjustment process. However, the bird can receive the rotation information from multiple magnetic particle arrangements or from other means (such as the gravity information response) to assist in navigation. Furthermore, the modulation patterns are very similar to the results obtained by radical-pair-based mechanism only,[7,8] but the biophysical

mechanisms are completely different.

6. Conclusion

In this paper we proposed a biophysical mechanism for magnetoreception in birds, which combines the magnetite- and radical-pair-based mechanisms to provide a more reasonable explanation of avian magnetoreception. The amplitude of the resultant magnetic field produced by the interaction between the magnetic particles and the geomagnetic field was analyzed using two materials with different magnetic properties. The relationship between the direction of the geomagnetic field and the radical-pair product yield was investigated. The calculation results show that the period of variation for singlet state product is approximately 180° when the magnetic particles are ferromagnetic materials, which could explain the experimental results of avian magnetic compass research. The singlet state products through the magnetic field in a reception plane are investigated. Their modulation patterns can provide geomagnetic information in birds. The model calculation results show that the proposed model, which deals with the magnetic particle role in changing the direction information of the geomagnetic field into the amplitude of the resultant magnetic field, can explain how birds use the geomagnetic field for navigation better than using either a magnetite- or radical-pair-based mechanism only.

Acknowledgment

The authors thank Dr. Xu Chun-Xiao for valuable discussion.

References

[1] Wiltschko W and Merkel F 1966 *Verh. dt. Zool. Ges.* **59** 362
[2] Johnsen S and Lohmann K J 2005 *Nat. Rev. Neurosci.* **6** 703
[3] Kirschvink J L, Kobayashikirschvink A, Diazricci J C and Kirschvink S J 1992 *Bioelectromagnetics* 101
[4] Cadiou H and McNaughton P A 2010 *J. R. Soc. Interface* **7** S193
[5] Shcherbakov V P and Winklhofer M 2010 *Phys. Rev. E* **81** 031921
[6] Schulten K, Swenberg C E and Weller A 1978 *Z. Phys. Chem. Neue. Fol.* **111** 1
[7] Ritz T, Adem S and Schulten K 2000 *Biophys. J.* **78** 707
[8] Solov'yov I A, Mouritsen H and Schulten K 2010 *Biophys. J.* **99** 40
[9] Blakemore R 1975 *Science* **190** 377
[10] Walker M M, Diebel C E, Haugh C V, Pankhurst P M, Montgomery J C and Green C R 1997 *Nature* **390** 371
[11] Eder S H K, Cadiou H, Muhamad A, McNaughton P A, Kirschvink J L and Winklhofer M 2012 *PNAS* **109** 12022
[12] Zhao J G, Wen G H, Liu C L, Liu C H and Zhan W S 1999 *Acta Phys. Sin.* **48** 973 (in Chinese)
[13] Kirschvink J L 1997 *Nature* **390** 339
[14] Kirschvink J L, Walker M M and Diebel C E 2001 *Curr. Opin. Neurobiol.* **11** 462
[15] Davila A F, Fleissner G, Winklhofer M and Petersen N 2003 *Phys. Chem. Earth.* **28** 647
[16] Fleissner G, Stahl B, Thalau P, Falkenberg G and Fleissner G 2007 *Naturwissenschaften.* **94** 631
[17] Solov'yov I A and Greiner W 2007 *Biophys. J.* **93** 1493
[18] Beason R C and Semm P 1987 *Neurosci. Lett.* **80** 229
[19] Beason R C and Semm P 1996 *J. Exp. Biol.* **199** 1241
[20] Leask M J M 1977 *Nature* **267** 144
[21] Wiltschko R and Wiltschko W 1998 *Naturwissenschaften.* **85** 164
[22] Wiltschko W, Munro U, Ford H and Wiltschko R 1993 *Nature* **364** 525
[23] Zapka M, Heyers D, Hein C M, Engels S, Schneider N L, Hans J, Weiler S, Dreyer D, Kishkinev D, Wild J M and Mouritsen H 2009 *Nature* **461** 1274
[24] Salikhov K M, Molin Y N, Sagdeev R A and Buchachenko A L 1984 *Elsevier.* **137** 51
[25] Steiner U E and Ulrich T 1989 *Chem. Rev.* **89** 51
[26] Timmel C R, Till U, Brocklehurst B, McLauchlan K A and Hore P J 1998 *Mol. Phys.* **95** 71
[27] Meng X G, Wang J S and Liang B L 2010 *Chin. Phys. B* **19** 044202
[28] Jia B Y, Yu Z Y, Liu Y M, Han L H, Yao W J, Feng H and Ye H 2011 *Chin. Phys. B* **20** 067301
[29] Timmel C R, Cintolesi F, Brocklehurst B and Hore P J 2001 *Chem. Phys. Lett.* **334** 387
[30] Rodgers C T and Hore P J 2009 *P. Natl. Acad. Sci.* USA **106** 353
[31] Ritz T, Ahmad M, Mouritsen H, Wiltschko R and Wiltschko W 2010 *J. R. Soc. Interface* **7** S135
[32] Lau J C S, Wagner-Rundell N, Rodgers C T, Green N J B and Hore P J 2010 *J. R. Soc. Interface* **7** S257
[33] Groff R P, Suna A, Avakian P and Merrifie R 1974 *Phys. Rev. B* **9** 2655
[34] Bube W, Michelbeyerle M E, Haberkorn R and Steffens E 1977 *Chem. Phys. Lett.* **50** 389
[35] Boxer S G, Chidsey C E D and Roelofs M G 1982 *P. Natl. Acad. Sci-Biol.* **79** 4632
[36] Vandijk B, Vandervos R and Hoff A J 1994 *Chem. Phys. Lett.* **226** 206
[37] Maeda K, Henbest K B, Cintolesi F, Kuprov I, Rodgers C T, Liddell P A, Gust D, Timmel C R and Hore P J 2008 *Nature* **453** 387
[38] Niessner C, Denzau S, Gross J C, Peichl L, Bischof H J, Fleissner G, Wiltschko W and Wiltschko R 2011 *Plos. One* **6** e20091
[39] Maeda K, Robinson A J, Henbest K B, Hogben H J, Biskup T, Ahmad M, Schleicher E, Weber S, Timmel C R and Hore P J 2012 *P. Natl. Acad. Sci.* USA **109** 4774
[40] Wiltschko W and Wiltschko R 2005 *J. Comp. Physiol. A* **191** 675
[41] Binhi V N 2006 *Bioelectromagnetics* **27** 58
[42] Binhi V N 2008 *Int. J. Radiat. Biol.* **84** 569
[43] Cohen A E 2009 *J. Phys. Chem. A* **113** 11084
[44] Yang N and Cohen A E 2010 *Opt. Express* **18** 25461
[45] Cai J M, Guerreschi G G and Briegel H J 2010 *Phys. Rev. Lett.* **104** 220502
[46] Mouritsen H and Hore P J 2012 *Curr. Opin. Neurobiol.* **22** 343
[47] Winklhofer M and Kirschvink J L 2010 *J. R. Soc. Interface* **7** S273
[48] Falkenberg G, Fleissner G, Schuchardt K, Kuehbacher M, Thalau P, Mouritsen H, Heyers D, Wellenreuther G and Fleissner G 2010 *Plos. One* **5** e9231
[49] Treiber C D, Salzer M C, Riegler J, Edelman N, Sugar C, Breuss M, Pichler P, Cadiou H, Saunders M, Lythgoe M, Shaw J and Keays D A 2012 *Nature* **484** 367
[50] Timmel C R and Henbest K B 2004 *Philos. T. Roy. Soc. A* **362** 2573
[51] Hoff A J and Hore P J 1984 *Chem. Phys. Lett.* **108** 104
[52] Mohtat N, Cozens F L, Hancock-Chen T, Scaiano J C, McLean J and Kim J 1998 *Photochem. Photobiol.* **67** 111
[53] Wiltschko W and Wiltschko R 1996 *J. Exp. Biol.* **199** 29